Post mortem interval estimation: features of cerebrospinal fluid films autofluorescent laser polarimetry

Bachynskyi V, Garazdiuk M, Vanchuliak O, Bezhenar I, Garazdiuk O

Higher State Educational Establishment of Ukraine "Bucovinian State Medical University", Chernivtsi, Ukraine

Abstract

Aim: The purpose of the work is development and testing of the two-dimensional Stokes-polarimetric mapping of biological layers own fluorescence to evaluate accuracy of the post-mortem interval (PMI) estimation using statistical analysis of postmortem changes dynamics of the coordinate distributions values of polycrystalline films of liquor (PFL) images laser-induced fluorescence polarisation intensity (LIFPI).
Methods: Objects of study are PFL, taken in 72 corpses with accurately known time of death and 20 healthy volunteers. The cause of the death was cardiovascular accident. Coordinate distributions of LIFPI image values were estimated for each sample of PFL in the optical arrangement of the Stokes polarimeter in different spectral bands of optical radiation.
The value of statistical points 1st – 4th order was performed for each two-dimensional distribution of PFL images LIFPI values. Statistical processing of the calculated values of set of points that characterise the LIFPI distributions within representative sampling was carry out. The depending on the time change of the most sensitive points of statistical values were built to achieve values stabilisation.
Results and conclusions: Two-dimensional Stokes-polarimetric mapping distributions LIFPI of PFL images may be used in determination of the PMI. Statistical points of the 1st and 3rd orders are the most sensitive PFL optical values to evaluate postmortem changes by different ranges of fluorescence.
Dynamic changes of PFL laser have demonstrated the effectiveness of the method to estimate PMI.

Keywords: post - mortem interval, cerebrospinal fluid, laser polarimetry, autofluorescence

Výpočet posmrtných intervalov: prvky na filmoch mozgovomiechového moku v autofluorescentnej laserovej polarimetrii

Abstrakt

Cieľ: Cieľom tejto práce je vývoj a testovanie dvojrozmerného polarimetrického mapovania autofluorescencie biologických vrstiev podľa Stokesa na vyhodnotenie presnosti výpočtu posmrtných intervalov (PMI) použitím štatistickej analýzy dynamiky hodnôt posmrtných zmien súradnicovej distribúcie snímok polykryštalických filmov likvoru (PFL) meraním laserom vyvolanej fluorescenčnej polarizačnej intenzity (LIFPI).
Metódy. Predmetom štúdie sú vzorky PFL zo 72 tiel s presne známym časom smrti a z dvadsiatich zdravých dobrovoľníkov. Smrť nastala v dôsledku kardiovaskulárnej príhody. Súradnicové distribúcie hodnôt LIFPI snímok sa odhadovali pre každú vzorku PFL s optickým usporiadaním polarimetra podľa Stokesa v rôznych spektrálnych pásmach optického žiarenia.
Hodnota 1.- 4. rádu štatistických bodov bola získaná pre každú dvojdimenzionálnu distribúciu PFL snímok LIFPI hodnôt. V rámci reprezentatívneho vzorkovania sa vykonalo štatistické spracovanie vypočítaných hodnôt súpravy bodov, ktoré charakterizuje distribúcie LIFPI. Na zastabilizovanie hodnôt sa vytvorila závislosť najcitlivejších bodov štatistických hodnôt od zmeny času.
Výsledky a závery. Dvojrozmerné distribúcie polarimetrického mapovania podľa Stokesa laserom indukovanej fluorescenčnej polarizačnej intenzity PFL snímok je možné využiť na stanovenie PMI. Štatistické body 1. a 3. rádu predstavujú pri stanovení posmrtných zmien pomocou rôznych rozsahov fluorescencie najcitlivejšie PFL optické hodnoty.
Dynamické zmeny PFL pri použití laseru preukázali efektívnosť metódy pri stanovení PMI.

Kľúčové slová: posmrtný interval, mozgovomiechový mok, laserová polarimetria, autofluorescencia

Corresponding Address:
2, Kyshynivska, str., 58001, Chernivtsi, Ukraine.
e-mail: sudmed@bsmu.edu.ua

Introduction

The issue of post-mortem interval (PMI) estimation always attracted both foreign and domestic scientists, because it is the important problem in forensic practice [2,3,6-12]. Considerable difficulties of accurate PMI estimation are related to impact of large number of both external and internal factors on posthumous processes development. The main method of PMI estimation is still estimation of early and late post-mortem changes degree. An experience and skills of the forensic expert are equally important. The results demonstrate incomplete, often subjective information with broad time frames of different types of biological tissues (BT) postmortem changes that can not adequately meet the needs of investigations.

Physical methods of BT changes evaluation, which use laser technology to study the dynamics of changes in the biocrystalline structure optical properties after death are the most perspective in this area [8,11,12]. Description of these properties based on optical phenomena such as static and dynamic scattering, diffraction and interference of optical fields. Polarisation methods provide new information about the morphological and optical-anisotropic structure of BT. It makes possible to establish a link between BT physiological condition and polarisative-phase images parameters of BT architectonics.

Currently, the possibility of objective PMI estimation is insufficiently studied by examining postmortem changes of the structure of microscopic images of laser-induced fluorescence of human biological fluids (BF).

Fluorescent optical-physical methods are widely and very effectively used in medical diagnostics. These methods are based on the use of fluorescence effects - secondary radiation of different molecular structures arising under short-wave optical radiation to BT or BF.

We used a technique that is based on excitation of avtofluorescence of biological molecules by laser radiation - a laser-induced fluorescence. This method allows to combine study sites in different spectral distributions of avtofluorescence intensity

The purpose of the work is development and testing of the two-dimensional Stokes-polarimetric mapping of biological layers own fluorescence to evaluate accuracy of the post-mortem interval (PMI) assessment using statistical analysis of postmortem changes dynamics of the coordinate distributions values of polycrystalline films of liquor (PFL) images laser-induced fluorescence polarisation (LIFP) intensity.

Methods

Objects of investigation are PFL, taken in 77 corpses of both sexes aged 33 to 91 year with accurately known time of death which ranged from 1 to 41 hours (the main research group), and 20 healthy volunteers (comparison group). The selection of liquor was carried out according to the Dehn, R. W et.al. (2013) by suboccipital puncture from great occipital tank of corpse and during spinal anesthesia performing for surgery preparation in healthy volunteers [4]. In main group liquor was selected from cadavers who died because of cardiovascular disease – 63 cases (81.82%), pulmonary tuberculosis - 8 cases (10.39%), gastrointestinal tumors - 6 cases (7.79%). According to the time since death next allocation: 1-8 hours - 15 cases (19.4%), 8-16 hours- 15 cases (19.4%), 16-24 hours- 16 cases (20.9%), 24-32 hours - 16 cases (20.9%), 32-40 hours - 15 cases (19.4%).

Liquor films formed in identical conditions by causing a drop of CSF in optically homogeneous glass. Drying of films were conducted at room temperature (t = 220C). Mathematical processing and analysis of PFL images to establish time-based dynamics of CSF postmortem changes was performed.

Autofluorescent laser polarimetry.

Figure 1 shows a laser-Stokes polarimeter circuit, which are modified for autofluorescent research of biological layers [8].

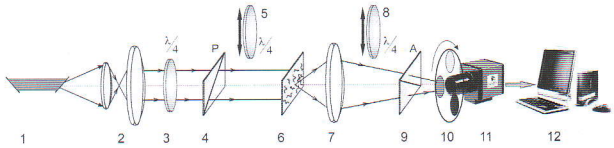

Fig. 1. Optical circuit of autofluorescence Stokes polarimeter. The explanation in the text.

PPL 6 irradiations regime consisted of parallel ($\text{Ø} = 2\times10^{3}\,\mu m$) bunch of "blue" ($\lambda_2 = 0.405\,\mu m$) semiconductor laser 1. Polarisation irradiator consists of two polarisation elements - quarter- wave plate 3 and polarisator 4. Image 6 PFL samples using polarisation object glass 7 (Nikon CFI Achromat P, the focal length - 30mm, aperture - 0.1, increase - 4x) was projected into the light-sensitive plane 10 of CCD-camera (The Imaging Source DMK 41AU02.AS, monochrome 1 / 2 "CCD, Sony ICX205AL (progressive scan); resolution - 1280x960; photosensitive plane size - 7600x6200mkm; sensitivity - 0.05 lx; dynamic range - 8 bit). PFL 6 samples polarisation analysis was carry out by the help of quarter- wave plate 8 and polarisator 9.

Thus, the main information objects for optic-physical methods set of PMI determination in our work are collection of directly measured coordinate distributions of PFL fluorescence

$$I_{ik}^{\Phi}(m \times n)$$

intensity:

$$I_{ik}^{\Phi}(m\times n)=\begin{pmatrix}(I_{ik}^{\Phi})_{11} & .. & (I_{ik}^{\Phi})_{1n}\\ . & .. & .\\ (I_{ik}^{\Phi})_{m1} & .. & (I_{ik}^{\Phi})_{mn}\end{pmatrix}; \quad (1)$$

The statistical moment of first (Z_1), second (Z_2), third (Z_3) and fourth (Z_4) orders were used as the main analytical tool to assess the PFL fluorescence intensity values distribution (further $q(m\times n)$). These moments were calculated according to the following algorithms [8,11,12]:

$$Z_1=\frac{1}{N}\sum_{j=1}^{N}q_j;$$
$$Z_2=\sqrt{\frac{1}{N}\sum_{j=1}^{N}(q^2)_j};$$
$$Z_3=\frac{1}{Z_2^3}\frac{1}{N}\sum_{j=1}^{N}(q^3)_j;$$
$$Z_4=\frac{1}{Z_2^4}\frac{1}{N}\sum_{j=1}^{N}(q^4)_j, \quad (2)$$

where "N" - the number of CCD-camera photosensitive area pixels.

Results

Posthumous dynamics of cerebrospinal fluid biophysical changes is largely depend on changes in proteins and their decay products [1]. Last ones are the consequence of free radical oxidation of proteins processes which has activated practically in case of any pathology intravitality. This phenomenon represents on PFL properties to refract light rays and laser beams. Accordingly, depending establishment of PFL laser polarimetric characteristics to PMI estimation can be applied for diagnostic purposes.

There are known the following fluorofores groups for the BT and BF which emit most intensely in different spectral:

1) the shortwavelength " dark blue - blue" spectrum Δλ=0,46±0,48 μm – proteins, NADH;

2) the mediawavelength "green - yellow" spectrum Δλ=0,52±0,54 μm - flavines and folic acides;

3) the longwavelenght "red" spectrum Δλ=0,58±0,66 μm - porphyrins.

Porphyrin fluorescence intensity greatly depends on the pH [5]. The fluorescence intensity increases by the pH increasing and conversely that observed in the postmortem processes course. As for NADH, in case when wavelenght is 450 nm, the autofluorescence is decreasing. We can assume that it is caused by the destruction of cells and therefore decrease of production NADH by them because of reducing the number of mitochondria. In the NADH transition to oxidized state it loses its ability to fluoresce. Reduced form of NAD has a characteristic absorption bands in the UV range (260 and 340 nm) and emission in the range 465-480 nm. In the NADH transition to oxidized state it is loses 340 nm absorption band and the ability to luminescence.

Flavin fluorescence depends strongly on the pH also. Flavin fluorescence absorption maxima are at 450 and 540 nm. Oxidized forms of flavoproteines exhibit fluorescence maximum of 520 nm and have characteristic absorption spectra (450, 375 and 263 nm) and luminescence (520-530 nm). They lose 450 nm absorption during the transition of these substances in restored condition.

1. The two-dimensional mapping of the ILIF distribution of molecular PFL in the short-range spectrum.

In carrying out ILIF distribution of values mapping the $\lambda_{max}^{(1)}=0{,}45 мкм$ bandpass filter with a peak bandwidth were used.

Experimental study of post-mortem biochemical structure changes temporal dynamics of PFL proteins and NADH for measuring ILIF coordinate distributions was performed by the following algorithm:

1. Blue semiconductor laser LSR405ML-LSR-PS-II emission with a wavelength λ=0,405 μm and power W=50mWt was applied for each PFL sample in the Stokes polarimeter optical arrangement (Fig. 1).
2. Spectral-selective two-dimensional PFL ILIF values distribution were measured due to a digital camera.
3. PFL images fluorescence maps measuring was performed in two stages. The first one - every 15 minutes during the first 6 hours after death. Second one every 30 minutes to 12 hours after death.
4. The value of statistical points of the 1 - 4 th order was performed for each two-dimensional distribution of PFL images ILIF values (equation (2)).
5. Statistical processing of the calculated values of set of points that characterise the PPL ILIF distributions within representative sampling was carried out.
6. The depending on the time change of the most sensitive to structure PFL fluorescent maps alteration statistical points were built for dynamic range of values "variation - stabilization".
7. The PMI and accuracy of time since death estimation were defined.

The examples of PFL images ILIF two-dimensional mapping in different time since death on the Figure2 and Figure 3 are represented.

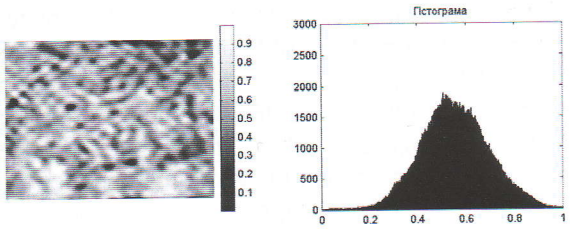

Fig. 2. Coordinate structure (left side) and distribution histogram (right side) of random values of PPL ILIF image. Time - 1 hour.

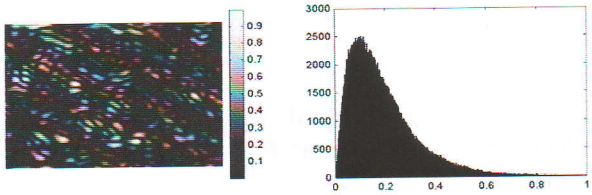

Fig. 3. Coordinate structure (left side) and distribution histogram (right side) of random values of PPL PE's image. Time - 6 hours.

The analysis of the data by ILIF mapping have found:

1. There is a distinct PFL proteins and NADH fluorescence dependence to PMI PPL in the "short-wave" spectrum. The change in the maximum intensity and range of spread in the histogram distribution has indicated in this fact (Fig. 2, Fig. 3, right part).
2. Concentration of proteins and NADH is rapidly decreasing due to PFL degenerative changes at the molecular level with increasing observation time after death.
3. Comparison of autofluorescence random values of distribution histograms (Fig. 2 and Fig. 3, right part) has shown that the ILIF extreme value decreased almost 5 times -

$$I^{\Phi}_{\max}(T = 1hours) = 0,5 \rightarrow I^{\Phi}_{\max}(T = 6hours) = 0,11$$

during 6 hours after death.

4. Statistical points of the 1st and the 3rd order are the most sensitive PFL optical values to evaluate postmortem changes. They characterize PFL images ILIF values mean and asymmetry distribution. Table 1.

T, hours.	1	4	8	12	18	24
Z_1	0,52 ± 0,038	0,63 ± 0,044	0,74 ± 0,058	0,91 ± 0,08	1,08 ± 0,09	1,25 ± 0,1
Z_4	0,85 ± 0,065	0,92 ± 0,072	1,08 ± 0,087	1,25 ± 0,1	1,44 ± 0,11	1,59 ± 0,13

Tab. 1. Time dependence of statistical points 1st and 3rd order which characterize the ILIF values distribution of protein and NADH molecules of PFL.

Statistical analysis of temporal dynamics of the PFL (proteins and NADH molecules) image ILIF map values distribution has found

1) the range of variation statistical values of the 1st order which characterizes the average value distribution PFL ILIF samples in the "blue" region of the spectrum is 2.4 times;
2) the range of variation statistical values of the 3rd order which characterizes the asymmetry value distribution PFL ILIF samples in the "blue" region of the spectrum is 1.87 times.

2. The two-dimensional mapping of the ILIF distribution of molecular PFL in the media-wavelength spectrum.

In carrying out ILIF distribution of values mapping $\lambda^{(2)}_{\max} = 0,55$ μm bandpass filter with a peak bandwidth were used.

The examples of PFL images ILIF two-dimensional mapping in different time since death, which ones shows the results of the postmortem changes monitoring of two-dimensional maps (left side) and histograms fluorescence intensity values (right side) in "green - yellow" section spectral range are represented on Fig.4 and Fig.5.

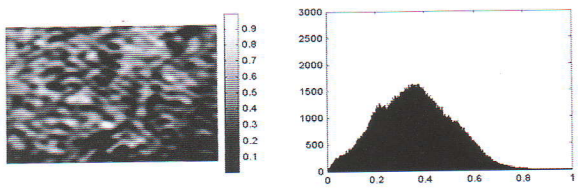

Fig. 4. Coordinate structure (left side) and distribution histogram (right side) of random values of PPL ILIF image in the media-wavelength spectrum. Time - 1 h.

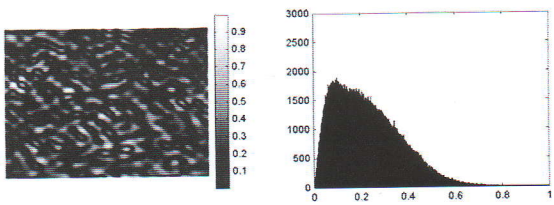

Fig. 5. Coordinate structure (left side) and distribution histogram (right side) of random values of PPL ILIF image in the media-wavelength spectrum. Time - 6 h.

From the data analysis of two-dimensional mapping obtained in the arrangement of Stokes-polarimeter with spectrally selective filtering of PFL images autofluorescence we can see fairly rapid decreasing of the intensity of secondary emission biochemical compounds in the medium section of the spectral range in the short (6 hours) time interval after death (Fig. 4 and Fig. 5, left side). The mean intensity significant changes of flavin and folic acid

autofluorescence (3.5 times) have illustrated this process quantitatively

$$I^{\Phi}_{\max}(T = 1hours) = 0,35 \rightarrow I^{\Phi}_{\max}(T = 6hours) = 0,095$$

in the distribution of the histograms (Fig. 4, Fig. 5, right side).

As a result, the time monitoring PFL molecular compounds postmortem changes in "green - yellow" section of the spectrum of optical emission statistical moments of the 1st and 3rd order, describing the average (Z_1) and asymmetry (Z_3) distribution of random values of the secondary emission of flavin and folic acid intensity, are the most dynamically changed - Table 2.

T, hours.	1	4	10	16	22	28
Z_1	0,56± 0,035	0,81± 0,063	0,97± 0,076	1,14± 0,11	1,31± 0,12	1,48± 0,13
Z_3	0,33± 0,021	0,51± 0,032	0,68± 0,044	0,85± 0,066	1,02± 0,092	1,19± 0,1

Tab. 2. Time dependence of statistical points 1st and 3rd order which characterize the ILIF values distribution of flavin and folic acid molecules of PFL.

3. The two-dimensional mapping of the ILIF distribution of molecular PFL in the long-range spectrum.

In carrying out ILIF distribution of values mapping $\lambda^{(3)}_{\max} = 0,63 мкм$, bandpass filter with a peak bandwidth were used fore porphirins. The research results of PFL images ILIF two-dimensional mapping PMI estimation in "red" section spectral range are represented on Fig.6 and Fig.7.

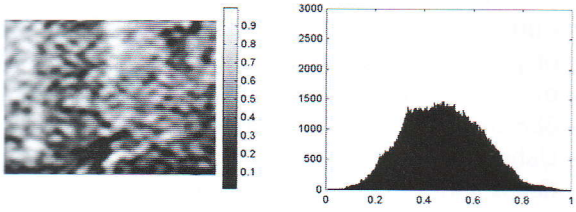

Fig. 6. Coordinate structure (left side) and distribution histogram (right side) of random values of PPL ILIF image in the long-range spectrum. Time - 1 h.

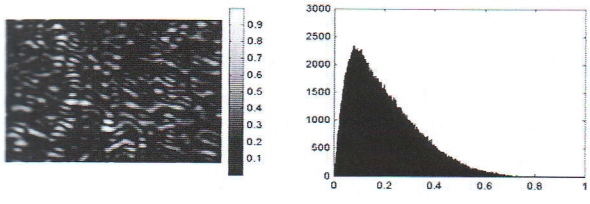

Fig. 7. Coordinate structure (left side) and distribution histogram (right side) of random values of PPL ILIF image in the long-range spectrum. Time - 3 h.

From the PFL two-dimensional autofluorescence mapping data analysis in different spectral bands and similar addictions that are obtained in the long-wavelength spectral range we can see greater sensitivity of optical displays of porphyrins molecular complexes data at different time of observation after death. Quantitatively, this fact illustrates significant changes (4 times decreasing) of the average spread of PFL porphyrins ILIF random values (Fig. 6, Fig. 7, right part) in the shortest (3 hours) period of time after death - Table 3.

T, hours	1	3	5	7	10	14
Z_1	0,54± 0,038	0,71± 0,05	0,88± 0,065	1,05± 0,085	1,22± 0,1	1,41± 0,11
Z_3	0,93± 0,076	1,11± 0,091	1,28± 0,097	1,45± 0,11	1,62± 0,13	1,79± 0,14

Tab. 3. Time dependence of statistical points 1st and 3rd order which characterize the ILIF values distribution of porphyrins molecules of PFL.

Statistical analysis of temporal dynamics of the PFL (porphyrins molecules) image ILIF map values distribution has found:

1) the range of variation statistical values of the 1st order which characterizes the average value distribution PFL ILIF samples in the "red" region of the spectrum is 2.6 times;
2) the range of variation statistical values of the 3rd order which characterizes the asymmetry value distribution PFL ILIF samples in the "red" region of the spectrum is 1.92 times.

Comparative analysis of the posthumous porphyrin autofluorescence temporal dynamics with data of two-dimensional proteins, NADH, flavin and folic acid fluorescent mapping, has found PMI interval estimation maximum reducing for a given optical-physical methods (T=14 hours) by the most rapid decrease of statistical points 1st and 3th order values.

Analytical algorithm to determine postmotrtem interval

Figure 8 illustrates algorithm of postmortem interval estimation

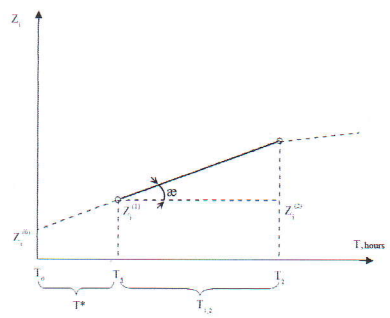

Fig. 8. Algorithm of postmortem interval determination. Here:

T_1 - time of value $Z_i^{(1)}$ measurement start;; T_2 - time of value $Z_i^{(2)}$ measurement end in the moment of its value ($Z_i^{(2)}(T) \approx const$); T_0 - time of death; ξ - inclination angle of informational dependence $Z_i(T)$.

After chart analysis we get the next equation to estimate interval:

$$tg\xi = \frac{Z_i^{(1)} - Z_i^{(1)}}{T_2 - T_1} = \frac{\Delta Z_i^{(1,2)}}{\Delta T_{12}} . \quad (3)$$

Using equation (3), we obtain the equation to estimate time since death:

$$T^* = Z_i^{(0)} \frac{\Delta T_{12}}{\Delta Z_i^{(1,2)}} . \quad (4)$$

Here: $Z_i^{(0)}$ - objective value, defined by a fence liquor collecting in vivo in healthy volunteers.

Conclusions

1. The two-dimensional mapping intensity distribution of laser-induced autofluorescence polycrystalline films of liquor method in postmortem changes time monitoring in different endogenous fluorophores biochemical molecular complexes for estimating the time since death in different spectral bands of optical emission was approved.
2. Optimal interval in 24 hours and the accuracy of the time since death estimation 25 min by short-wavelenght fluorescence for proteins and NADH molecules were estimated.
3. Optimal interval in 28 hours and the accuracy of the time since death determination 35 min by medium-wavelenght fluorescence for flavines and folioacides molecules
4. Optimal interval in 14 hours and the accuracy of the time since death determination 15 min by long-wavelenght fluorescence for porphyrins molecules

References

1. Aksjonova, V. M., & Starkova, A. V. (1998). Diagnosticheskaja cennost' opredelenija urovnja veshhestv srednej molekuljarnoj massy v plazme novorozhdjonnyh detej, perenjosshih vnutriutrobnuju gipoksiju. Perm. med. zhurnal, 15(1), 25-28.
2. Arroyo, A., Rosel, P., & Marron, T. (2005). Cerebrospinal fluid: postmortem biochemical study. Journal of clinical forensic medicine, 12(3), 153-156. doi: 10.1016/j.jflm.2015.09.017.
3. Chen, J. H., Inamori-Kawamoto, O., Michiue, T., Ikeda, S., Ishikawa, T., & Maeda, H. (2015) Cardiac biomarkers in blood, and pericardial and cerebrospinal fluids of forensic autopsy cases: A reassessment with special regard to postmortem interval. Legal Medicine (Tokyo). 2015 Sep; 17(5): 343-50. doi: 10.1016/j.legalmed. 2015.03.007. Epub 2015 Apr 30.
4. Dehn, R. W., & Asprey, D. P. (2013). Essential Clinical Procedures: Expert Consult-Online and Print. Elsevier Health Sciences. P. 146-156.
5. Erythrocyte Protoporphyrin Fluorescence as a Biomarker for Monitoring Antiangiogenic Cancer Therapy/ De Goes Rocha, F. G. Barbosa Chaves, K. C. Gomes // Journal of fluorescence.- 2010. - 20(6) - 1225-1231.
6. Estimation of postmortem interval through albumin in CSF by simple dye binding method / A.K. Parmar, S.K. Menon // Sci Justice. – 2015. - 55(6) – P. 388-393. doi: 10.1016/j.scijus. 2015.07.005
7. Finehout, E. J., Franck, Z., Relkin, N., & Lee, K. H. (2006). Proteomic analysis of cerebrospinal fluid changes related to postmortem interval. Clinical chemistry, Oct; 52(10):1906-13. Epub 2006 Aug 3.
8. Fourier polarimetry of the birefringence distribution of myocardium tissue / O.G. Ushenko, O.V. Dubolazov, V.O. Ushenko [et al] // Proc. SPIE. – 2015. – Vol. 9809. - P. 980915-980915. - doi:10.1117/12.2228980.
9. Girela, E., Villanueva, E., Irigoyen, P., Girela, V., Hernández-Cueto, C., & Peinado, J. M. (2008). Free amino acid concentrations in vitreous humor and cerebrospinal fluid in relation to the cause of death and postmortem interval. Journal of forensic sciences, 2008 May; 53(3):730-3. doi: 10.1111/j.1556-4029.2008.00726.x.
10. Parmar, A. K., & Menon, S. K. (2015). Estimation of postmortem interval through albumin in CSF by simple dye binding method. *Sci Justice, 55*(6), 388-393. doi: 10.1016/j.scijus.2015.07.005
11. Ushenko, O. G., Dubolazov, O. V., Ushenko, Y. O., & Gorsky, M. P. (2015, November). Scale-selective analysis of myocardium polarisation images in problems of diagnostic of necrotic changes. In 12th International Conference on Correlation Optics (pp. 98091C-98091C). International Society for Optics and Photonics. doi:10.1117/12.2228998.
12. Ushenko, V. O., Olar, O. V., Ushenko, Y. O., Gorsky, M. P., & Soltys, I. V. (2015, November). Polarisation correlometry of polycrystalline films of human liquids in problems of forensic medicine. In 12th International Conference on Correlation Optics (pp. 98091B-98091B). International Society for Optics and Photonics. doi:10.1117/12.2228997.